Physics Letters B 778 (2018) 178–183

Contents lists available at ScienceDirect

Physics Letters B

www.elsevier.com/locate/physletb

Isospin-symmetry breaking in masses of $N \simeq Z$ nuclei

P. Bączyk [a,*], J. Dobaczewski [a,b,c,d], M. Konieczka [a], W. Satuła [a,d], T. Nakatsukasa [e], K. Sato [f]

[a] Institute of Theoretical Physics, Faculty of Physics, University of Warsaw, ul. Pasteura 5, PL-02-093 Warsaw, Poland
[b] Department of Physics, University of York, Heslington, York YO10 5DD, United Kingdom
[c] Department of Physics, P.O. Box 35 (YFL), University of Jyväskylä, FI-40014 Jyväskylä, Finland
[d] Helsinki Institute of Physics, P.O. Box 64, FI-00014 University of Helsinki, Finland
[e] Center for Computational Sciences, University of Tsukuba, Tsukuba 305-8577, Japan
[f] Department of Physics, Osaka City University, Osaka 558-8585, Japan

ARTICLE INFO

Article history:
Received 13 November 2017
Received in revised form 19 December 2017
Accepted 22 December 2017
Available online 17 January 2018
Editor: J.-P. Blaizot

Keywords:
Nuclear density functional theory (DFT)
Energy density functional (EDF)
Proton–neutron mixing
Isospin symmetry breaking (ISB)
Mirror displacement energy (MDE)
Triplet displacement energy (TDE)

ABSTRACT

Effects of the isospin-symmetry breaking (ISB) beyond mean-field Coulomb terms are systematically studied in nuclear masses near the $N = Z$ line. The Coulomb exchange contributions are calculated exactly. We use extended Skyrme energy density functionals (EDFs) with proton–neutron-mixed densities, to which we add new terms breaking the isospin symmetry. Two parameters associated with the new terms are determined by fitting mirror and triplet displacement energies (MDEs and TDEs) of isospin multiplets. The new EDFs reproduce MDEs for the $T = \frac{1}{2}$ doublets and $T = 1$ triplets, and TDEs for the $T = 1$ triplets. Relative strengths of the obtained isospin-symmetry-breaking terms *are not* consistent with the differences in the NN scattering lengths, a_{nn}, a_{pp}, and a_{np}. Based on low-energy experimental data, it seems thus impossible to delineate the strong-force ISB effects from beyond-mean-field Coulomb-energy corrections.

1. Introduction

Similarity between the neutron–neutron (nn), proton–proton (pp), and neutron–proton (np) nuclear forces, commonly known as their charge independence, has been well established experimentally already in 1930's, leading to the concept of the isospin symmetry introduced by Heisenberg [1] and Wigner [2]. Since then, the isospin symmetry has been tested and widely used in theoretical modeling of atomic nuclei, with its explicit violation generated by the Coulomb interaction. In addition, there also exists firm experimental evidence in the nucleon–nucleon (NN) scattering data that the interaction contains small isospin-symmetry-breaking (ISB) components. The differences in the NN phase shifts indicate that the nn interaction, V_{nn}, is about 1% stronger than the pp interaction, V_{pp}, and that the np interaction, V_{np}, is about 2.5% stronger than the average of V_{nn} and V_{pp} [3]. These effects are called charge-symmetry breaking (CSB) and charge-independence breaking (CIB), respectively. In this Letter, we show that the manifestation of the CSB and CIB in nuclear masses can systematically be accounted for by the extended nuclear density functional theory (DFT).

The charge dependence of the nuclear strong force fundamentally originates from mass and charge differences between u and d quarks. The strong and electromagnetic interactions among these quarks give rise to the mass splitting among the baryonic and mesonic multiplets. The neutron is slightly heavier than the proton. The pions, which are the Goldstone bosons associated with the chiral symmetry breaking and are the primary carriers of the nuclear force at low energy, also have the mass splitting. The strong-force CSB mostly originates from the difference in masses of protons and neutrons, leading to the difference in the kinetic energies and influencing the one- and two-boson exchange. On the other hand, the major cause of the strong-force CIB is the pion mass splitting. For more details, see Refs. [3,4].

The Coulomb force is, of course, the major source of ISB in nuclei. In the nuclear DFT, the Coulomb interaction is treated on the mean-field level. Contrary to the atomic DFT, where the exchange and correlation effects are usually treated together [5], in nuclei, the exchange term can be evaluated exactly, as is the case in the present study, but the correlation terms are simply disregarded. Therefore, the ISB terms that we introduce below are meant to describe both the strong-force and Coulomb-correlation effects jointly.

The isospin formalism offers a convenient classification of different components of the nuclear force by dividing them into

* Corresponding author.
E-mail address: pawel.baczyk@fuw.edu.pl (P. Bączyk).

https://doi.org/10.1016/j.physletb.2017.12.068

four distinct classes. Class-I isoscalar forces are invariant under any rotation in the isospin space. Class-II isotensor forces break the charge independence but are invariant under a rotation by π with respect to the y-axis in the isospace preserving therefore the charge symmetry. Class-III isovector forces break both the charge independence and the charge symmetry, and are symmetric under interchange of two interacting particles. Finally, forces of class IV break both symmetries and are anti-symmetric under the interchange of two particles. This classification was originally proposed by Henley and Miller [4,6] and subsequently used in the framework of potential models based on boson-exchange formalism, like CD-Bonn [3] or AV18 [7]. The CSB and CIB were also studied in terms of the chiral effective field theory [8,9]. So far, the Henley-Miller classification has been rather rarely utilized within the nuclear DFT [10,11], which is usually based on the isoscalar strong forces.[1]

The most prominent manifestation of the ISB is in the mirror displacement energies (MDEs) defined as the differences between binding energies of mirror nuclei:

$$\mathrm{MDE} = BE(T, T_z = -T) - BE(T, T_z = +T). \tag{1}$$

A systematic study by Nolen and Schiffer [12] showed that the MDEs cannot be reproduced by using models involving mean-field Coulomb interaction as the only source of the ISB, see also Refs. [11,13–15]. Another source of information on the ISB are the so-called triplet displacement energies (TDEs):

$$\mathrm{TDE} = BE(T=1, T_z=-1) + BE(T=1, T_z=+1) - 2BE(T=1, T_z=0), \tag{2}$$

which are measures of the binding-energy curvatures within the isospin triplets. The TDEs cannot be reproduced by means of conventional approaches disregarding nuclear CIB forces either, see [13,16]. In the above definitions of MDEs and TDEs, the binding energies are negative ($BE < 0$) and the proton (neutron) has isospin projection of $t_z = -\frac{1}{2}(+\frac{1}{2})$, that is, $T_z = \frac{1}{2}(N - Z)$.

In Fig. 1, we show MDEs and TDEs calculated fully self-consistently using three different standard Skyrme energy-density functionals (EDFs): $\mathrm{SV_T}$ [17,18], SkM* [19], and SLy4 [20]. Details of the calculations, performed using code HFODD [21], are presented in the Supplemental Material [22]. In Fig. 1(a), we clearly see that the values of obtained MDEs are systematically lower than the experimental ones by about 10%. Even more spectacular discrepancy appears in Fig. 1(b) for TDEs, namely, for the $A = 4n$ triplets their values are nicely reproduced by the mean-field Coulomb effects, however, the characteristic staggering pattern seen in experiment is entirely absent. (See below for the discussion regarding the outlier case of ^{44}V.) It is also very clear that the calculated MDEs and TDEs, which are specific differences of binding energies, are independent of the choice of Skyrme EDF parametrization, that is, of the isoscalar part of the EDF.

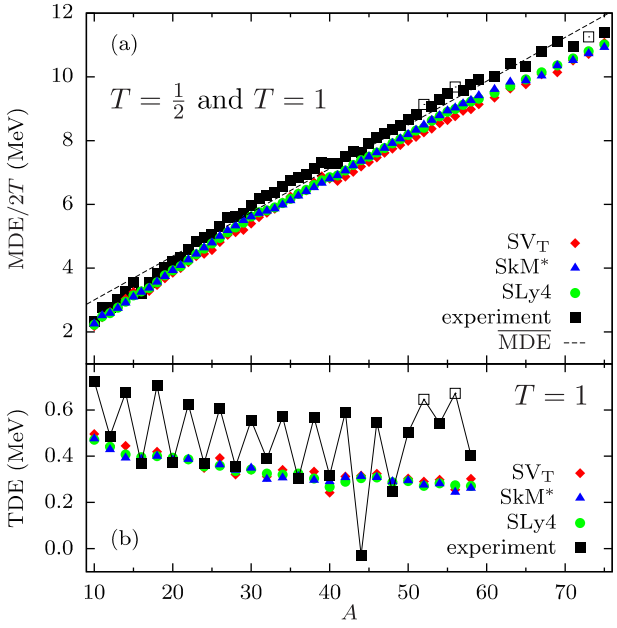

Fig. 1. (Color online.) Calculated (no ISB terms) and experimental values of MDEs (a) and TDEs (b). The values of MDEs for triplets are divided by two to fit in the plot. Thin dashed line shows the average linear trend of experimental MDEs in doublets, defined as $\overline{MDE} = 0.137A + 1.63$ (in MeV). Measured values of binding energies were taken from Ref. [25] and the excitation energies of the $T = 1$, $T_z = 0$ states from Ref. [26]. Open squares denote data that depend on masses derived from systematics [25].

2. Methods

We aim at a comprehensive study of MDEs and TDEs based on the extended Skyrme *pn*-mixed DFT [21,27,28], which includes zero-range class-II and III forces. We consider the following zero-range interactions of class II and III with two new low-energy coupling constants t_0^{II} and t_0^{III} [29]:

$$\hat{V}^{\mathrm{II}}(i,j) = t_0^{\mathrm{II}}\,\delta(\boldsymbol{r}_i - \boldsymbol{r}_j)\left[3\hat{\tau}_3(i)\hat{\tau}_3(j) - \hat{\vec{\tau}}(i)\circ\hat{\vec{\tau}}(j)\right], \tag{3}$$

$$\hat{V}^{\mathrm{III}}(i,j) = t_0^{\mathrm{III}}\,\delta(\boldsymbol{r}_i - \boldsymbol{r}_j)\left[\hat{\tau}_3(i) + \hat{\tau}_3(j)\right]. \tag{4}$$

The corresponding contributions to EDF read:

$$\mathcal{H}_{\mathrm{II}} = \frac{1}{2}t_0^{\mathrm{II}}(\rho_n^2 + \rho_p^2 - 2\rho_n\rho_p - 2\rho_{np}\rho_{pn} - \boldsymbol{s}_n^2 - \boldsymbol{s}_p^2 + 2\boldsymbol{s}_n\cdot\boldsymbol{s}_p + 2\boldsymbol{s}_{np}\cdot\boldsymbol{s}_{pn}), \tag{5}$$

$$\mathcal{H}_{\mathrm{III}} = \frac{1}{2}t_0^{\mathrm{III}}\left(\rho_n^2 - \rho_p^2 - \boldsymbol{s}_n^2 + \boldsymbol{s}_p^2\right), \tag{6}$$

where ρ and $\boldsymbol{s}$ are scalar and spin (vector) densities, respectively. Inclusion of the spin exchange terms in Eqs. (3) and (4) leads to a trivial rescaling of coupling constants t_0^{II} and t_0^{III}, see [29]. Hence, these terms were disregarded.

Contributions of class-III force to EDF (6) depend on the standard *nn* and *pp* densities and, therefore, can be taken into account within the conventional *pn*-separable DFT approach [10,11]. In contrast, contributions of class-II force (5) depend explicitly on the mixed densities, ρ_{np} and $\boldsymbol{s}_{np}$, and require the use of *pn*-mixed DFT [27,28].

We implemented the new terms of the EDF in the code HFODD [21], where the isospin degree of freedom is controlled within the isocranking method [27,30,31] – an analogue of the cranking technique that is widely used in high-spin physics. The isocranking method allows us to calculate the entire isospin multiplet, T, by starting from an isospin-aligned state $|T, T_z = T\rangle$ and isocranking it around axes tilted with respect to the z-axis. In particular, the isocranking around the x-axis (or equivalently around the y-axis) allows us to reach the state with $\langle\hat{T}_z\rangle \simeq 0$. We note here that the analogy between cranking and isocranking is not

[1] In this Letter, we use terms isoscalar, isovector, and isotensor, which pertain to the covariance of the total interaction or functional with respect to rotations in the isospace. These names are confusingly identical to terms isoscalar and isovector that are used in the nuclear DFT to describe parts of the functional that depend on the isoscalar or isovector densities, respectively. Both standards are now widely used in the literature, but they should not be confused.

perfect. Indeed, the former term is most often used for spatially deformed states, where the tilted cranking refers to the cranking axes not coinciding with the principal axes of the mass distribution. Since in the isospace there is no analogue of the deformation, we can only speak about the isocranking axes tilted with respect to the z-axis, which is the symmetry axis of the Coulomb force.

A rigorous treatment of the isospin symmetry within the pn-mixed DFT formalism requires full, three-dimensional isospin projection, which is currently under development. However, for the purpose of calculating values of TDEs, we can perform the isospin projection in the following way. First, we treat the standard effects of the isospin mixing caused by the Coulomb interaction at the mean-field level, cf. [32]. That is, we consider mean-field states of nuclei with $(T, T_z = \pm 1)$ as having approximately good isospin. Then, the only states that need special attention are those with $(T, T_z = 0)$, which are obtained by the isocranking technique.

Let us denote by $|\Psi_{T,Tz}\rangle = \{|\Psi_{1,-1}\rangle, |\Psi_{1,0}\rangle, |\Psi_{1,1}\rangle\}$ the wavefunctions of the triplet of states. For the $A = 4n + 2$ triplets, these wave functions can be very simply written as

$$\begin{aligned} |\Psi_{1,-1}\rangle &= a^+_{p\uparrow} a^+_{p\downarrow} |0\rangle, \\ |\Psi_{1,0}\ \rangle &= \frac{1}{\sqrt{2}} \left(a^+_{n\uparrow} a^+_{p\downarrow} + a^+_{p\uparrow} a^+_{n\downarrow} \right) |0\rangle, \\ |\Psi_{1,1}\ \rangle &= a^+_{n\uparrow} a^+_{n\downarrow} |0\rangle, \end{aligned} \tag{7}$$

where $\uparrow$ and $\downarrow$ denote pairs of Kramers-degenerate deformed states, and $|0\rangle$ denotes the $T = 0$ core of $A = 4n$ particles.

Similarly, the x-isocranked state reads

$$|\Psi_{++}\rangle = a^+_{+\uparrow} a^+_{+\downarrow} |0\rangle = \tfrac{1}{2} |\Psi_{1,-1}\rangle + \tfrac{1}{\sqrt{2}} |\Psi_{1,0}\rangle + \tfrac{1}{2} |\Psi_{1,1}\rangle, \tag{8}$$

where $|+\uparrow\rangle = \frac{1}{\sqrt{2}} (|n\uparrow\rangle + |p\uparrow\rangle)$ and $|+\downarrow\rangle = \frac{1}{\sqrt{2}} (|n\downarrow\rangle + |p\downarrow\rangle)$ are single-particle eigenstates of the Pauli matrix τ_x. Since all terms in the Hamiltonian are diagonal in T_z, we then have the binding energy of the isocranked state as $BE_{++} = \frac{1}{4} BE(T = 1, T_z = -1) + \frac{1}{2} BE(T = 1, T_z = 0) + \frac{1}{4} BE(T = 1, T_z = +1)$. When this result is inserted into Eq. (2), we finally obtain[2]

$$\mathrm{TDE} = 2 \Big[BE(T = 1, T_z = -1) + BE(T = 1, T_z = +1) - 2BE_{++} \Big]. \tag{9}$$

For the $A = 4n$ triplets, the derivation is slightly more involved, but the same result (9) holds. In this way, TDEs of the isospin-projected triplets can be determined from energies of three Slater determinants: $|\Psi_{1,-1}\rangle$, $|\Psi_{++}\rangle$, and $|\Psi_{1,1}\rangle$. The procedure proposed in Eqs. (7)–(9) is equivalent to an exact projection on the $N = Z$ $T = 1$ component of the isocranked wavefunction, which amounts to removing its dispersion in T_z.

Physically relevant values of t_0^{II} and t_0^{III} turn out to be fairly small [29], that is, of the order of a few MeV fm^3 as compared to the values of the isoscalar parameter t_0, which are typically larger than 1000 MeV fm^3. Therefore, the new terms do not impair the overall agreement of self-consistent results with the standard experimental data. Moreover, calculated MDEs and TDEs depend on t_0^{II} and t_0^{III} almost linearly, and, in addition, MDEs (TDEs) depend very weakly on t_0^{II} (t_0^{III}) [22,29]. This allows us to use the standard linear regression method, see, e.g. Refs. [35,36], to independently adjust t_0^{II} and t_0^{III} to experimental values of TDEs and MDEs, respectively. See Supplemental Material [22] for detailed description of the procedure. Coupling constants t_0^{II} and t_0^{III} resulting from such an adjustment are collected in Table 1. We have performed adjustments to masses tabulated in AME2012 [25]; in this way, below we can test our predictions by comparing the results to those tabulated in AME2016 [37].

[2] In Refs. [23,29,33,34], we have erroneously used Eq. (2) with $BE(T = 1, T_z = 0)$ replaced by BE_{++}, which resulted in numerical values of TDEs being twice too small, cf. Eq. (9), and in incorrect values of the adjusted coupling constants t_0^{II}.

Table 1
Coupling constants t_0^{II} and t_0^{III} and their uncertainties obtained in this work for the Skyrme EDFs SV$_{\mathrm{T}}^{\mathrm{ISB}}$, SkM$^{*\mathrm{ISB}}$, and SLy4$^{\mathrm{ISB}}$. In the last row we show their corresponding ratios.

	SV$_{\mathrm{T}}^{\mathrm{ISB}}$	SkM$^{*\mathrm{ISB}}$	SLy4$^{\mathrm{ISB}}$
t_0^{II} (MeV fm^3)	4.6 ± 1.6	7 ± 4	6 ± 4
t_0^{III} (MeV fm^3)	-7.4 ± 1.9	-5.6 ± 1.4	-5.6 ± 1.1
$t_0^{\mathrm{II}}/t_0^{\mathrm{III}}$	-0.6 ± 0.3	-1.3 ± 0.8	-1.1 ± 0.7

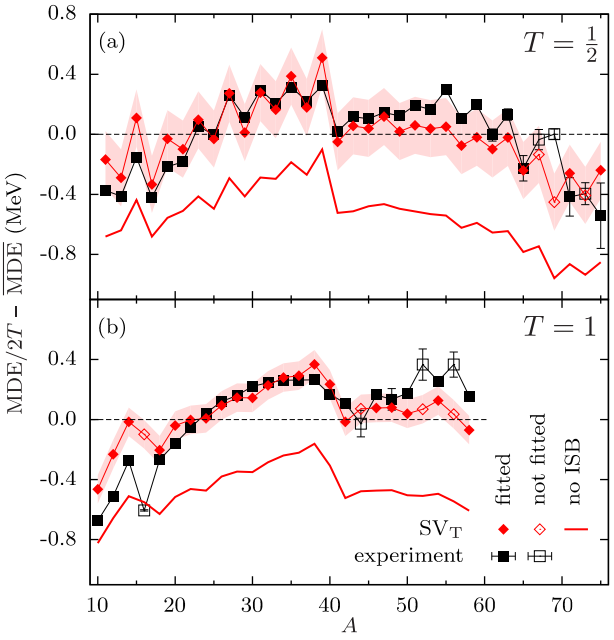

Fig. 2. (Color online.) Calculated and experimental [25] values of MDEs for the $T = \frac{1}{2}$ (a) and $T = 1$ (b) mirror nuclei, shown with respect to the average linear trend defined in Fig. 1. Calculations were performed for functional SV$_{\mathrm{T}}^{\mathrm{ISB}}$. Shaded bands show theoretical uncertainties, evaluated according to the methodology discussed in detail in the Supplemental Material [22]. Experimental error bars are shown only when they are larger than the corresponding symbols. Full (open) symbols denote data points included in (excluded from) the fitting procedure.

3. Results

In Fig. 2, we show values of MDEs calculated within our extended DFT formalism for the Skyrme SV$_{\mathrm{T}}^{\mathrm{ISB}}$ EDF. By subtracting an overall linear trend (as defined in Fig. 1) we are able to show results in an extended scale, for which a detailed comparison with experimental data is possible. In Fig. 3, we show the corresponding SV$_{\mathrm{T}}^{\mathrm{ISB}}$ values of TDEs, whereas complementary results obtained for the Skyrme SkM$^{*\mathrm{ISB}}$ and SLy4$^{\mathrm{ISB}}$ EDFs are collected in the Supplemental Material [22]. Here, we concentrate on the results given by the Skyrme SV$_{\mathrm{T}}^{\mathrm{ISB}}$ EDF, because it is the only one based on averaging a two-body pseudopotential (without density-dependent terms), and it is thus free from unwanted self-interaction contributions [38].

It is gratifying to see that the calculated values of MDEs closely follow the experimental A-dependence, see Fig. 2. It is worth noting that a single coupling constant t_0^{III} reproduces both $T = \frac{1}{2}$ and $T = 1$ MDEs, which confirms conclusions of Refs. [10,11]. In addition, for the $T = \frac{1}{2}$ MDEs, Fig. 2(a), the SV$_{\mathrm{T}}^{\mathrm{ISB}}$ results nicely re-

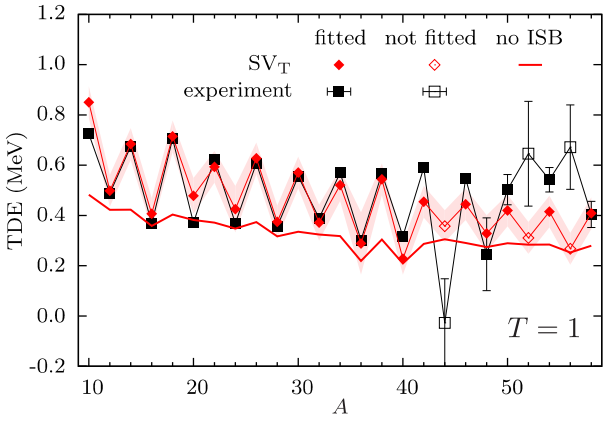

Fig. 3. (Color online.) Same as in Fig. 2 but for the $T = 1$ TDEs with no linear trend subtracted.

produce (i) changes in experimental trend that occur at $A = 15$ and 39, (ii) staggering pattern between $A = 15$ and 39, and (iii) quenching of staggering between $A = 41$ and 53 (the $f_{7/2}$ nuclei).

We note that these features are already present in the SV$_T$ results without the ISB terms, that is, for the mean-field Coulomb interaction. On top of the Coulomb force, the class-III force is essential in bringing the magnitude of MDEs up to the experimental values, but also in simultaneously *increasing* the staggering pattern given by the Coulomb interaction. This is illustrated in Fig. 4(a), where we plotted differences MDE(A)−MDE($A-2$), separately for the contributions coming from the isoscalar, Coulomb, and class-III terms of the functional.

On the one hand, we see that the Coulomb force alone always induces staggering of MDEs, except in the $f_{7/2}$ and $g_{9/2}$ nuclei, where this part of the staggering disappears almost completely. On the other hand, the class-III force induces a (smaller) *in-phase* staggering in all systems. Because of the self-consistency, the isoscalar terms also show some small out-of-phase staggering, which is a result of strong cancellation between fairly large kinetic-energy and Skyrme-force contributions. In Fig. 4(b), we showed differences MDE(A)−MDE($A-2$) calculated with and without the ISB terms, compared with experimental values [25]. This figure also shows results of our calculations extrapolated up to $A = 99$.

For all three functionals our results correctly describe the A-dependence, and lack of staggering, of the $T = 1$ MDEs, see Fig. 2(b) and [22]. Coming to the discussion of TDEs, it is even more gratifying to see in Fig. 3 that our pn-mixed calculations, with one adjusted class-II coupling constant, $t_0^{\rm II}$, describe absolute values and staggering of TDEs quite well. By including the class-II force into the SV$_T$ parametrization, the overall rms deviations of TDEs decreases from 190 to 69 keV. In fact, the improvement comes from the decrease of the rms deviations for the $A = 4n + 2$ triplets, from 250 to 75 keV, wheres those for the $A = 4n$ triplets change very little, from 58 to 60 keV.

We also note that (i) in our approach, the staggering of MDEs in the $f_{7/2}$ shell is increased by the ISB terms, leading to an agreement with data, Fig. 4(b), whereas in the results of Ref. [14] this staggering is decreased by the ISB forces. Also, (ii) in light of our results, the standard interpretation of a phenomenological term in Coulomb energies [12,39] that is proportional to $(-1)^Z$, is not correct. This term was introduced to remove effects of the proton Coulomb self-energies. Our calculations treat the Coulomb-exchange terms exactly, and thus are free from self-energies; nevertheless, these exact Coulomb energies do not show any staggering of the TDEs, Fig. 3. Therefore, our results disprove the motivation for introducing a phenomenological $(-1)^Z$ term that generates a uniform staggering of MDEs and TDEs. And (iii) for the

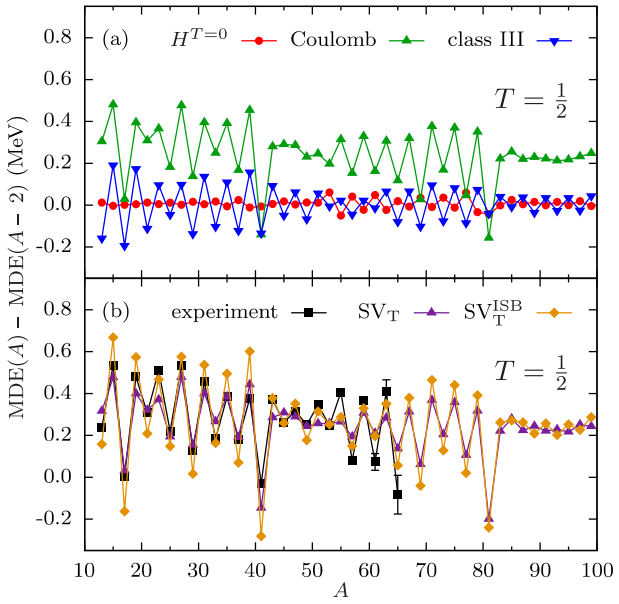

Fig. 4. (Color online.) Staggering of the calculated $T = \frac{1}{2}$ MDEs: MDE(A)−MDE($A-2$). (a) Separate contributions of the isoscalar ($H^{T=0}$), Coulomb, and class-III terms, determined for functional SV$_T^{\rm ISB}$. (b) Results obtained for functionals SV$_T$ (no ISB) and SV$_T^{\rm ISB}$ (fitted) compared with experimental data [25].

SkM*$^{\rm ISB}$ and SLy4$^{\rm ISB}$ functionals, the staggering of the $T = \frac{1}{2}$ MDEs and TDEs is less pronounced than for SV$_T^{\rm ISB}$ [22] and the results obtained without the ISB terms show almost no staggering in $T = \frac{1}{2}$ MDEs. This may suggest that the staggering of Coulomb energies in $T = \frac{1}{2}$ MDEs may be washed out by the self-interaction contributions, which are present in the SkM*$^{\rm ISB}$ and SLy4$^{\rm ISB}$ functionals due to explicit density dependence [38].

Good agreement obtained for the MDEs and TDEs shows that the role and magnitude of the simplest DFT ISB terms are now firmly established. Nevertheless, some conspicuous deviations of our theoretical predictions with respect to the experiment still remain. This includes (i) overestimated (underestimated) values of MDEs in lighter (heavier) multiplets, (ii) overestimated (underestimated) staggering of MDEs in lighter (heavier) doublets, and (iii) underestimated staggering of TDEs in heavier triplets. This suggests that higher-order DFT ISB terms, that is, gradient terms that would generate dependence on surface properties, may still play some role.

It is very instructive to look at ten outliers that were excluded from the fitting procedure. In Figs. 2 and 3, they are shown by open symbols. They can be classified as (i) five outliers that depend on masses of ^{52}Co, ^{56}Cu, and ^{73}Rb, which clearly deviate from the calculated trends for MDEs and TDEs. These masses were not directly measured but were derived from systematics [25]. And (ii) two outliers that depend on the mass of ^{44}V, whose ground-state measurement may be contaminated by an unresolved isomer [40–42]. As well as (iii), large differences between experimental and calculated values are found in MDE for $A = 16$, 67 and 69. Inclusion of these data in the fitting procedure would significantly increase the uncertainty of adjusted coupling constants. The former two classes of outliers, (i) and (ii), call for improving experimental values, whereas the last one (iii) may be a result of structural effects not included in our model.

Our results can be confronted with the state-of-the-art global analysis performed within the shell-model [13]. There, the MDEs and TDEs were very accurately described by fitting the Coulomb, class-II, and class-III shell-model interactions, separately in five different valence spaces between $A = 10$ and 55. In addition, values

Table 2
Mass excesses of ^{52}Co, ^{56}Cu, ^{73}Rb, and ^{44}V obtained in this work and compared with those of AME2012 [25] and AME2016 [37]. Our predictions were calculated as weighted averages of values obtained from MDEs and TDEs for all three used Skyrme parametrizations. The AME values derived from systematics are labeled with symbol #.

Nucleus	Mass excess (keV)		
	This work	AME2012 [25]	AME2016 [37]
^{52}Co	−34370(40)	−33990(200)#	−34361.0(84)
^{56}Cu	−38650(40)	−38240(200)#	−38643(15)
^{73}Rb	−46100(80)	−46080(100)#	−46080(200)#
^{44}V	−23710(40)	−24120(180)	−24120(180)

of 14 single-particle energies were also adjusted. As a result of such a 29-parameter fit, the rms deviations between measured and calculated values of MDEs and TDEs were obtained as 44 and 23 keV, respectively. This can be contrasted with our two-parameter fit in $\mathrm{SV}_{\mathrm{T}}^{\mathrm{ISB}}$, resulting in the corresponding rms deviations of 220 and 66 keV. (Here, we have used the same set of nuclei as that analyzed in Ref. [13].) Undoubtedly, this shows that by adding higher-order DFT ISB terms, our results can still be improved. Nevertheless, we can conclude that both the DFT and shell-model analyses consistently point to the necessity of using specific ISB terms to account for masses of $N \simeq Z$ nuclei.

Having at hand a model with the ISB interactions included, we can calculate MDEs and TDEs for more massive multiplets, and make predictions of binding energies for neutron-deficient ($T_z = -T$) nuclei. In particular, in Table 2 we present predictions of mass excesses of ^{52}Co, ^{56}Cu, and ^{73}Rb, whose masses were in AME2012 [25] derived from systematics, and ^{44}V, whose ground-state mass measurement is uncertain. Recently, the mass excess of ^{52}Co was measured as −34361(8) [43] or −34331.6(66) keV [44]. These values are in excellent agreement with our prediction, even though the difference between them is still far beyond the estimated (much smaller) experimental uncertainties. We also note that a similar excellent agreement is obtained between our mass excess of ^{56}Cu and that of AME2016 [37]. On the other hand, estimates given in Ref. [42] are outside our error bars.

Assuming that the extracted CSB and CIB effects are, predominantly, due to the ISB in the $^1S_0$ NN scattering channel, one can attempt relating ratio $t_0^{\mathrm{II}}/t_0^{\mathrm{III}}$ to the experimental scattering lengths. The reasoning follows the work of Suzuki et al. [10], who assumed a proportionality between the strengths of CSB and CIB forces and the corresponding scattering lengths [45], that is, $V_{CSB} \propto \Delta a_{CSB} = a_{pp} - a_{nn}$ and $V_{CIB} \propto \Delta a_{CIB} = \frac{1}{2}(a_{pp} + a_{nn}) - a_{np}$, which, in our case, is equivalent to $t_0^{\mathrm{III}} \propto -\frac{1}{2}\Delta a_{CSB}$ and $t_0^{\mathrm{II}} \propto \frac{1}{3}\Delta a_{CIB}$. Assuming further that the proportionality constant are the same, and taking for the experimental values $\Delta a_{CSB} = 1.5 \pm 0.3$ fm and $\Delta a_{CIB} = 5.7 \pm 0.3$ fm [45], one gets the estimate:

$$\frac{t_0^{\mathrm{II}}}{t_0^{\mathrm{III}}} = -\frac{2}{3}\frac{\Delta a_{CIB}}{\Delta a_{CSB}} = -2.5 \pm 0.5. \tag{10}$$

From the values of coupling constants t_0^{II} and t_0^{III} obtained in this work, we can obtain their ratios as given in Table 1. As we can see, the ratios determined by our analysis of masses of $N \simeq Z$ nuclei with $10 \leq A \leq 75$ have a correct sign but are 2–4 times smaller than the estimate (10) based on properties of the NN forces deduced from the NN scattering experiments.

4. Conclusions

In this Letter, we showed that the nuclear DFT with added two new terms related to the ISB interactions of class II and III is able to systematically reproduce observed MDEs and TDEs of $T = \frac{1}{2}$ and $T = 1$ multiplets. Adjusting only two coupling constants, t_0^{II} and t_0^{III}, we reproduced not only the magnitudes of the MDE and TDE but also their characteristic staggering patterns. The obtained values of t_0^{II} and t_0^{III} turn out to *not agree* with the NN ISB interactions (NN scattering lengths) in the $^1S_0$ channel. We predicted mass excesses of ^{52}Co, ^{56}Cu, ^{73}Rb, and ^{44}V, and for ^{52}Co and ^{56}Cu we obtained excellent agreement with the recently measured values [37,43,44]. To better pin down the ISB effects, accurate mass measurements of the other two nuclei are very much called for.

Our work constitutes the first global DFT study of TDEs in the $T = 1$ isomultiplets. It is based on the introduction of a single class-II ISB term within the *pn*-mixed DFT [27,28]. In addition, we confirmed results of Refs. [10,11], which described the values of MDEs by using a single class-III ISB term. We also showed that the characteristic staggering patterns of MDEs are mostly related to the standard Coulomb effects, whereas those of TDEs require introducing the class-II ISB terms. Altogether, we showed that very simple general DFT ISB terms properly account for all currently available experimental data for MDEs and TDEs.

Finally, we note that our adjusted ISB terms probably jointly include effects of the Coulomb correlations beyond mean field and ISB strong interactions, along with possible many-body ISB correlations induced by them. It does not seem reasonable to expect that low-energy nuclear experimental data would allow for disentangling these distinct sources of the ISB in finite nuclei. In this respect, *ab initio* derivations, such as recently performed for four triplets in Ref. [16], would be very important, provided they cover the entire set of data available experimentally.

Interesting comments by Witek Nazarewicz are gratefully acknowledged. This work was supported in part by the Polish National Science Center under Contract Nos. 2014/15/N/ST2/03454 and 2015/17/N/ST2/04025, by the Academy of Finland and University of Jyväskylä within the FIDIPRO program, by Interdisciplinary Computational Science Program in CCS, University of Tsukuba, by ImPACT Program of Council for Science, Technology and Innovation (Cabinet Office, Government of Japan), and by JSPS and NSFC under the Japan-China Scientific Cooperation Program. We acknowledge the CIŚ Świerk Computing Center, Poland, and the CSC-IT Center for Science Ltd., Finland, for the allocation of computational resources.

Appendix A. Supplementary material

Supplementary material related to this article can be found online at https://doi.org/10.1016/j.physletb.2017.12.068.

References

[1] W. Heisenberg, Über den Bau der Atomkerne, Z. Phys. 77 (1932) 1.
[2] E. Wigner, On the consequences of the symmetry of the nuclear hamiltonian on the spectroscopy of nuclei, Phys. Rev. 51 (1937) 106–119, https://doi.org/10.1103/PhysRev.51.106, URL http://link.aps.org/doi/10.1103/PhysRev.51.106.
[3] R. Machleidt, High-precision, charge-dependent Bonn nucleon–nucleon potential, Phys. Rev. C 63 (2001) 024001, https://doi.org/10.1103/PhysRevC.63.024001, URL https://link.aps.org/doi/10.1103/PhysRevC.63.024001.
[4] G.A. Miller, W.H.T. van Oers, Symmetries and Fundamental Interactions in Nuclei, World Scientific, 1995.
[5] R.G. Parr, W. Yang, Density-Functional Theory of Atoms and Molecules, Oxford University Press, New York, 1989.
[6] E.M. Henley, G.A. Miller, Mesons in Nuclei, North Holland, 1979.
[7] R.B. Wiringa, S. Pastore, S.C. Pieper, G.A. Miller, Charge-symmetry breaking forces and isospin mixing in ^{8}Be, Phys. Rev. C 88 (2013) 044333, https://doi.org/10.1103/PhysRevC.88.044333, URL http://link.aps.org/doi/10.1103/PhysRevC.88.044333.
[8] M. Walzl, U.-G. Meißner, E. Epelbaum, Charge-dependent nucleon–nucleon potential from chiral effective field theory, Nucl. Phys. A 693 (3–4) (2001) 663–692, https://doi.org/10.1016/S0375-9474(01)00969-1, URL http://www.sciencedirect.com/science/article/pii/S0375947401009691.

[9] E. Epelbaum, H.-W. Hammer, U.-G. Meißner, Modern theory of nuclear forces, Rev. Mod. Phys. 81 (2009) 1773–1825, https://doi.org/10.1103/RevModPhys.81.1773, URL https://link.aps.org/doi/10.1103/RevModPhys.81.1773.

[10] T. Suzuki, H. Sagawa, N. Van Giai, Charge independence and charge symmetry breaking interactions and the Coulomb energy anomaly in isobaric analog states, Phys. Rev. C 47 (1993) R1360–R1363, https://doi.org/10.1103/PhysRevC.47.R1360, URL http://link.aps.org/doi/10.1103/PhysRevC.47.R1360.

[11] B.A. Brown, W.A. Richter, R. Lindsay, Displacement energies with the Skyrme Hartree–Fock method, Phys. Lett. B 483 (1–3) (2000) 49–54, https://doi.org/10.1016/S0370-2693(00)00589-X, URL http://www.sciencedirect.com/science/article/pii/S037026930000589X.

[12] J.A. Nolen Jr, J.P. Schiffer, Coulomb energies, Annu. Rev. Nucl. Sci. 19 (1969) 471, https://doi.org/10.1146/annurev.ns.19.120169.002351, URL http://www.annualreviews.org/doi/abs/10.1146/annurev.ns.19.120169.002351.

[13] W. Ormand, B. Brown, Empirical isospin-nonconserving Hamiltonians for shell-model calculations, Nucl. Phys. A 491 (1) (1989) 1–23, https://doi.org/10.1016/0375-9474(89)90203-0, URL http://www.sciencedirect.com/science/article/pii/0375947489902030.

[14] K. Kaneko, Y. Sun, T. Mizusaki, S. Tazaki, Variation in displacement energies due to isospin-nonconserving forces, Phys. Rev. Lett. 110 (2013) 172505, https://doi.org/10.1103/PhysRevLett.110.172505, URL http://link.aps.org/doi/10.1103/PhysRevLett.110.172505.

[15] G. Colò, H. Sagawa, N. Van Giai, P.F. Bortignon, T. Suzuki, Widths of isobaric analog resonances: a microscopic approach, Phys. Rev. C 57 (1998) 3049–3054, https://doi.org/10.1103/PhysRevC.57.3049, URL http://link.aps.org/doi/10.1103/PhysRevC.57.3049.

[16] W.E. Ormand, B.A. Brown, M. Hjorth-Jensen, Realistic calculations for c coefficients of the isobaric mass multiplet equation in $1p0f$ shell nuclei, Phys. Rev. C 96 (2017) 024323, https://doi.org/10.1103/PhysRevC.96.024323, URL https://link.aps.org/doi/10.1103/PhysRevC.96.024323.

[17] M. Beiner, H. Flocard, N.V. Giai, P. Quentin, Nuclear ground-state properties and self-consistent calculations with the Skyrme interaction: (i). Spherical description, Nucl. Phys. A 238 (1) (1975) 29–69, https://doi.org/10.1016/0375-9474(75)90338-3, URL http://www.sciencedirect.com/science/article/pii/0375947475903383.

[18] W. Satuła, J. Dobaczewski, Simple regularization scheme for multireference density functional theories, Phys. Rev. C 90 (2014) 054303, https://doi.org/10.1103/PhysRevC.90.054303, URL https://link.aps.org/doi/10.1103/PhysRevC.90.054303.

[19] J. Bartel, P. Quentin, M. Brack, C. Guet, H.-B. Håkansson, Towards a better parametrisation of Skyrme-like effective forces: a critical study of the SkM force, Nucl. Phys. A 386 (1) (1982) 79–100, https://doi.org/10.1016/0375-9474(82)90403-1, URL http://www.sciencedirect.com/science/article/pii/0375947482904031.

[20] E. Chabanat, P. Bonche, P. Haensel, J. Meyer, R. Schaeffer, A Skyrme parametrization from subnuclear to neutron star densities Part II. Nuclei far from stabilities, Nucl. Phys. A 635 (1) (1998) 231–256, https://doi.org/10.1016/S0375-9474(98)00180-8, URL http://www.sciencedirect.com/science/article/pii/S0375947498001808.

[21] N. Schunck, J. Dobaczewski, W. Satuła, P. Bączyk, J. Dudek, Y. Gao, M. Konieczka, K. Sato, Y. Shi, X. Wang, T. Werner, Solution of the Skyrme–Hartree–Fock–Bogolyubov equations in the Cartesian deformed harmonic-oscillator basis. (VIII) HFODD (v2.73y): a new version of the program, Comput. Phys. Commun. 216 (2017) 145–174, https://doi.org/10.1016/j.cpc.2017.03.007, URL http://www.sciencedirect.com/science/article/pii/S0010465517300942.

[22] See Supplemental Material at https://doi.org/10.1016/j.physletb.2017.12.068, which includes Refs. [23,24], for details of the calculations performed using code HFODD, description of the fitting procedure, and results obtained for the Skyrme SkM* and SLy4 EDFs.

[23] P. Bączyk, J. Dobaczewski, M. Konieczka, T. Nakatsukasa, K. Sato, W. Satuła, Mirror and triplet displacement energies within nuclear DFT: numerical stability, Acta Phys. Pol. B 48 (2017) 259, https://doi.org/10.5506/APhysPolB.48.259.

[24] W. Satuła, J. Dobaczewski, W. Nazarewicz, T.R. Werner, Isospin-breaking corrections to superallowed Fermi β decay in isospin- and angular-momentum-projected nuclear density functional theory, Phys. Rev. C 86 (2012) 054316, https://doi.org/10.1103/PhysRevC.86.054316, URL https://link.aps.org/doi/10.1103/PhysRevC.86.054316.

[25] M. Wang, G. Audi, A.H. Wapstra, F.G. Kondev, M. MacCormick, X. Xu, B. Pfeiffer, The AME2012 atomic mass evaluation (II). Tables, graphs and references, Chin. Phys. C 36 (12) (2012) 1603–2014, URL http://amdc.in2p3.fr/masstables/Ame2012/Ame2012b-v2.pdf.

[26] Evaluated nuclear structure data file, http://www.nndc.bnl.gov/ensdf/.

[27] K. Sato, J. Dobaczewski, T. Nakatsukasa, W. Satuła, Energy-density-functional calculations including proton–neutron mixing, Phys. Rev. C 88 (2013) 061301, https://doi.org/10.1103/PhysRevC.88.061301, URL https://link.aps.org/doi/10.1103/PhysRevC.88.061301.

[28] J.A. Sheikh, N. Hinohara, J. Dobaczewski, T. Nakatsukasa, W. Nazarewicz, K. Sato, Isospin-invariant Skyrme energy-density-functional approach with axial symmetry, Phys. Rev. C 89 (2014) 054317, https://doi.org/10.1103/PhysRevC.89.054317, URL http://link.aps.org/doi/10.1103/PhysRevC.89.054317.

[29] P. Bączyk, J. Dobaczewski, M. Konieczka, W. Satuła, Strong-interaction isospin-symmetry breaking within the density functional theory, Acta Phys. Pol. B, Proc. Suppl. 8 (3) (2016) 539–544, https://doi.org/10.5506/APhysPolBSupp.8.539.

[30] W. Satuła, R. Wyss, Rotations in isospace: a doorway to the understanding of neutron–proton superfluidity in $N = Z$ nuclei, Phys. Rev. Lett. 86 (2001) 4488–4491, https://doi.org/10.1103/PhysRevLett.86.4488, URL http://link.aps.org/doi/10.1103/PhysRevLett.86.4488.

[31] W. Satuła, R. Wyss, Microscopic structure of fundamental excitations in $N = Z$ nuclei, Phys. Rev. Lett. 87 (2001) 052504, https://doi.org/10.1103/PhysRevLett.87.052504, URL http://link.aps.org/doi/10.1103/PhysRevLett.87.052504.

[32] W. Satuła, J. Dobaczewski, W. Nazarewicz, M. Rafalski, Isospin-symmetry restoration within the nuclear density functional theory: formalism and applications, Phys. Rev. C 81 (2010) 054310, https://doi.org/10.1103/PhysRevC.81.054310, URL http://link.aps.org/doi/10.1103/PhysRevC.81.054310.

[33] W. Satuła, J. Dobaczewski, M. Konieczka, W. Nazarewicz, Isospin mixing within the symmetry restored density functional theory and beyond, Acta Phys. Pol. B 45 (2014) 167, https://doi.org/10.5506/APhysPolB.45.167.

[34] P. Bączyk, J. Dobaczewski, M. Konieczka, W. Satuła, T. Nakatsukasa, K. Sato, Strong-force isospin-symmetry breaking in masses of $N \sim Z$ nuclei, arXiv:1701.04628v2, URL https://arxiv.org/abs/1701.04628v2.

[35] J. Toivanen, J. Dobaczewski, M. Kortelainen, K. Mizuyama, Error analysis of nuclear mass fits, Phys. Rev. C 78 (2008) 034306, https://doi.org/10.1103/PhysRevC.78.034306, URL https://link.aps.org/doi/10.1103/PhysRevC.78.034306.

[36] J. Dobaczewski, W. Nazarewicz, P.-G. Reinhard, Error estimates of theoretical models: a guide, J. Phys. G, Nucl. Part. Phys. 41 (7) (2014) 074001, URL http://stacks.iop.org/0954-3899/41/i=7/a=074001.

[37] M. Wang, G. Audi, F. Kondev, W. Huang, S. Naimi, X. Xu, The AME2016 atomic mass evaluation (ii). Tables, graphs and references, Chin. Phys. C 41 (3) (2017) 030003, URL http://stacks.iop.org/1674-1137/41/i=3/a=030003.

[38] D. Tarpanov, J. Toivanen, J. Dobaczewski, B.G. Carlsson, Polarization corrections to single-particle energies studied within the energy-density-functional and quasiparticle random-phase approximation approaches, Phys. Rev. C 89 (2014) 014307, https://doi.org/10.1103/PhysRevC.89.014307, URL https://link.aps.org/doi/10.1103/PhysRevC.89.014307.

[39] S. Shlomo, Nuclear Coulomb energies, Rep. Prog. Phys. 41 (7) (1978) 957, URL http://stacks.iop.org/0034-4885/41/i=7/a=001.

[40] Y. Fujita, T. Adachi, H. Fujita, A. Algora, B. Blank, M. Csatlós, J.M. Deaven, E. Estevez-Aguado, E. Ganioğlu, C.J. Guess, J. Gulyás, K. Hatanaka, K. Hirota, M. Honma, D. Ishikawa, A. Krasznahorkay, H. Matsubara, R. Meharchand, F. Molina, H. Okamura, H.J. Ong, T. Otsuka, G. Perdikakis, B. Rubio, C. Scholl, Y. Shimbara, E.J. Stephenson, G. Susoy, T. Suzuki, A. Tamii, J.H. Thies, R.G.T. Zegers, J. Zenihiro, High-resolution study of $T_z = +2 \rightarrow +1$ Gamow–Teller transitions in the ^{44}Ca(^{3}He,t)^{44}Sc reaction, Phys. Rev. C 88 (2013) 014308, https://doi.org/10.1103/PhysRevC.88.014308, URL http://link.aps.org/doi/10.1103/PhysRevC.88.014308.

[41] M. MacCormick, G. Audi, Evaluated experimental isobaric analogue states from to and associated IMME coefficients, Nucl. Phys. A 925 (2014) 61–95, https://doi.org/10.1016/j.nuclphysa.2014.01.007, URL http://www.sciencedirect.com/science/article/pii/S0375947414000220.

[42] X. Tu, Y. Litvinov, K. Blaum, B. Mei, B. Sun, Y. Sun, M. Wang, H. Xu, Y. Zhang, Indirect mass determination for the neutron-deficient nuclides 44V, 48Mn, 52Co and 56Cu, Nucl. Phys. A 945 (2016) 89–94, https://doi.org/10.1016/j.nuclphysa.2015.09.016, URL http://www.sciencedirect.com/science/article/pii/S0375947415002237.

[43] X. Xu, P. Zhang, P. Shuai, R.J. Chen, X.L. Yan, Y.H. Zhang, M. Wang, Y.A. Litvinov, H.S. Xu, T. Bao, X.C. Chen, H. Chen, C.Y. Fu, S. Kubono, Y.H. Lam, D.W. Liu, R.S. Mao, X.W. Ma, M.Z. Sun, X.L. Tu, Y.M. Xing, J.C. Yang, Y.J. Yuan, Q. Zeng, X. Zhou, X.H. Zhou, W.L. Zhan, S. Litvinov, K. Blaum, G. Audi, T. Uesaka, Y. Yamaguchi, T. Yamaguchi, A. Ozawa, B.H. Sun, Y. Sun, A.C. Dai, F.R. Xu, Identification of the lowest $T = 2$, $J^\pi = 0^+$ isobaric analog state in ^{52}Co and its impact on the understanding of β-decay properties of ^{52}Ni, Phys. Rev. Lett. 117 (2016) 182503, https://doi.org/10.1103/PhysRevLett.117.182503, URL http://link.aps.org/doi/10.1103/PhysRevLett.117.182503.

[44] D.A. Nesterenko, A. Kankainen, L. Canete, M. Block, D. Cox, T. Eronen, C. Fahlander, U. Forsberg, J. Gerl, P. Golubev, J. Hakala, A. Jokinen, V.S. Kolhinen, J. Koponen, N. Lalović, C. Lorenz, I.D. Moore, P. Papadakis, J. Reinikainen, S. Rinta-Antila, D. Rudolph, L.G. Sarmiento, A. Voss, J. Äystö, High-precision mass measurements for the isobaric multiplet mass equation at $A = 52$, J. Phys. G, Nucl. Part. Phys. 44 (6) (2017) 065103, URL http://stacks.iop.org/0954-3899/44/i=6/a=065103.

[45] G.A. Miller, B.M.K. Nefkens, I. Šlaus, Charge symmetry, quarks and mesons, Phys. Rep. 194 (1) (1990) 1–116, https://doi.org/10.1016/0370-1573(90)90102-8, URL http://www.sciencedirect.com/science/article/pii/0370157390901028.